International Journal of Chemistry and Material Science Vol. 2(2), pp. 028-045, June, 2014
Available online at http://academeresearchjournals.org/journal/ijcms
ISSN 2327-5553 ©2014 Academe Research Journals

Full Length Research Paper

Dosimetric characterization and spectroscopic study of radiochromic films as natural dye dosimeters

Muhammad Attique Khan Shahid[1]*, Bushra Bashir[1], Hina Bashir[2], Huma Bashir[1] and Arfa Mubashir[1]

[1]Department of Physics, G.C. University, Faisalabad, Punjab, Pakistan.
[2]Department of Zoology, Wild Life and Fisheries, G.C. University, Faisalabad, Punjab, Pakistan.

Accepted 28 April, 2014

Radiochromic films were prepared with PVA gel matrix and natural dyes (Turmeric, Walnut and Henna) with three concentrations, that is, C_1=0.5 g/L, C_2=0.25 g/L and C_3=0.13 g/L having pH value 4 for acidic samples and 10 for alkaline samples. The thickness of the film was fixed to be 0.05 mm. The behavior of the dyes was studied on the basis of change in specific absorbance with concentration, change in specific absorbance with absorbed dose; effect of pH on specific absorbance, electrical conductivity, molar extinction coefficients, and percentage decoloration. Absorption spectra for un-irradiated and Gamma irradiated films were studied. λ_{max} for T= 451 nm, for W=340 nm and for H=320 nm was recorded. Absorbance at each λ_{max} was found by using spectrophotometer and specific absorbance was calculated. Response curve for specific absorbance versus concentration showed linear behavior for each dye. Plot of specific absorbance versus dose made the behavior of the dye clear and it was noticed that acidic samples of all the dye samples worked best. Maximum degree of decoloration in the Turmeric, Walnut and Henna dye films was observed to be 94%, 51.5% and 93.7% respectively. XRD analysis was performed and it was found that for Turmeric, %age crystallanity as well as C.I decreased while for Walnut and Henna both factors increased. Moreover, mechanical properties of dye films were studied which showed that due to irradiation some changes had occurred in the crystal structure which is the major reason of decoloration of the dye films.

Key words: Irradiation, PVA Turmeric films, alkaline, acidic, optical and structural changes, mechanical properties, XRD study, dye dosimetry.

INTRODUCTION

Dye dosimetry is based on the fact that ionizing radiations interact with matter and cause the color change of the dye. This property of color change of dye can be used for dosimetry as the decomposition of dye is linear with respect to the amount of dose absorbed (Parwate et al., 2007; Al-Zahrany, 2011; Blaskov et al., 2011; Chen et al., 2008). The high energy ionizing radiations bring the radiolysis of the dye (decoloration or bleaching effect) which is used to measure the energy of the radiation incident on the chemical system.

The natural dyes are the source of strong, beautiful, stable and long-lasting colors. They are economical and cost-effective, ecofriendly, less toxic and less allergic. They are unsophisticated and coherent with nature, cause lower level of emission than synthetic dyes. Natural dyes are the most eco-friendly for the planet. Practically, no or minor chemical reactions are involved (Teli et al., 1994; Baha et al., 2011, 2012).

*Corresponding author. E-mail: profkhan786@yahoo.com.

NOMENCLATURE

XRD: X-ray diffraction; **PVA:** Polyvinyl Alcohol; **T-PVA:** Turmeric Polyvinyl Alcohol; **W-PVA:** Walnut Polyvinyl Alcohol; **H-PVA:** Henna Polyvinyl Alcohol; **Fsd:** Faisalabad; **EC:** Electrical Conductivity.

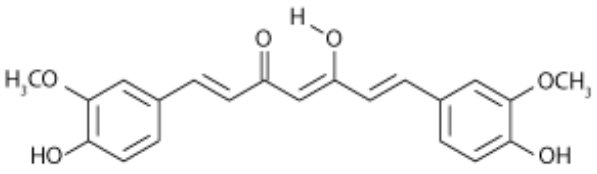

Figure 1. Structural sketch of turmeric dye.
1,7-bis(4-hydroxy-3-methoxyphenyl)-1, 6-heptadiene-3, 5-dione.

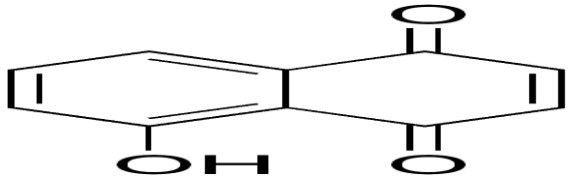

Figure 2. Structural sketch of walnut dye.
5-hydroxy1,4-naphthalenedione or 5-hydroxynaphthoquinone.

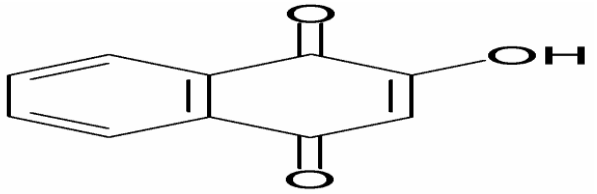

Figure 3. Structural sketch of henna dye.
2-hydroxy-1, 4-naphthoquinone.

Turmeric

Curcuma Longa is a small perennial herb native to India bearing many rhizomes on its root system which are the source of its culinary spice known as Turmeric and its medicinal extract called Curcumin. In addition to its popularity as a spice, turmeric is used as a dye or cloth and coloring agent in food and cosmetics.

Turmeric is mainly valued for its principal coloring constituent curcumin, which imparts the yellow color on textile fibers and food items. Rhizome, the main source of curcumin also contains various ingredients like protein, fat, fibers, carbohydrates, essential oil, etc. Curcumin possesses various bioactive properties and is used in modern system of medicine. It is well recognized for anti-inflammtory, hepatoprotective, anticancer, metabolic disorders, antimicribial, antiviral and antioxident activities (Sachin and Kapoor, 2007).

Walnut

Black walnut is a tree, native to North America. They served a very pivotal role in the food and lifestyle of the early colonial shelters and people used the outer covering of the nuts and bark of the tree to make medicines. The walnut tree has always been revered due to its long life which is several times that of humans and also because of versatile uses as food, medicine, housing, dye and lamp oil. Black walnut contains high concentration of chemical substance called tannins which is the major coloring constituent which imparts brown color. Walnuts are beneficial for heart and circulatory system. They help to maintain the proper blood composition. Walnuts contain omega-3 fatty acids and alpha linolenic acid (ALA). These acids help control cardiovascular functions including blood pressure, prevent cholesterol, and maintain blood sugar level. Anti-inflammatory properties of walnuts help to protect bone health. These are also effective for curing asthma, eczema and rheumatoid arthritis (Buttery et al., 2000; Wongcharee et al., 2007; Calogero and Marco, 2008; Wang et al., 2009). The schematic chemical structures found in literature are shown in Figures 1, 2 and 3.

Henna

Henna is a plant; its leaves are used to prepare medicines. The active coloring constituent of henna leaf is lawsone (0.5-1%). Other constituents are 5-10% galic acid, tannins and xanthone are some of the other contents of henna leaves. The lawsone is basically responsible for the coloring property of henna leaves. Henna is sometimes applied directly to the affected area for fungal infections, wounds, and dandruff and eczema scabies. Henna has been used for several diseases such as severe diarrhea caused by parasites, cancer, headache, jaundice and skin conditions. People have been taking henna for stomach and intestinal ulcers. As a cosmetic, henna is used as hair dyes and in hair care products, and as a dye for hands, nails and clothing.

Radiochromic films have been used as dose monitors in radiation processing dosimetry for the last 30 years. Dye films or sheets and dye precursors have been used as high dose monitors for the routine measurements of absorbed dose in food irradiation, sterilization of medical instruments and several other applications (Mehta et al., 1995; Basfar et al., 2011).

This study is focused on developing a film dosimeter with natural materials, having good dosimetric characteristics for routine dosimetry. New and novel materials and suitable read out techniques for their evaluation are desirable. The objective of this research is to prepare natural dye based PVA films to observe the decoloration of dye films on irradiation from Cs-137 Gamma source. The characteristics of dosimeter on the basis of physio-chemical changes like pH, molar extinction coefficient, EC with absorbed dose were determined to find out the correlation between color degradation and absorbed dose. Moreover, the use of XRD for the characterization of the film dosimeter is the

Table 1. Working conditions for XRD.

X-Radiation	NI-Filtered
X-ray Tube Voltage and Current	35 KV and 20mA
Divergent and anti-scatter slits	1°
Receiving slit	0.13 mm and 0.3 mm
Goniometer scanning speed/step width	$1°min^{-1}/0.02°$
Rate-meter time constant	1 s
Detector	Scintillation Counter
Start angle	70°
Stop angle	5°

ovelty of this project. Internal structure damage (crystallanity) was studied using X-ray diffraction (XRD), and optimum range for an ideal dosimeter fit for commercial purposes was suggested.

MATERIALS AND METHODS

The dried rhizomes of turmeric, walnut bark and henna leaves were crushed into powder form. Dye extract was prepared by taking 25 gm powder of the dye and dissolve it in 500 ml of distilled water to make a homogenous solution. This solution was refluxed for 1 h. The process was repeated thrice. Then the filtrate was dried with a rotary evaporator at reduced pressure to get the dye extracts (Ali et al., 2008). The T-PVA, W-PVA and H-PVA radiochromic dye films were prepared by using polyvinyl alcohol (PVA) (C_2H_4O, molecular weight: 44.04-108 g/mol) containing turmeric dye extracts ($C_{21}H_{20}O_6$, MW: 368.3 g/mol), walnut ($C_{10}H_6O_3$, MW: 174.16 g/mol) and henna ($C_{10}H_6O_3$, MW: 174.16 g/mol). 3 gm of PVA was dissolved in 50 ml of doubly distilled water to prepare a stock gel polymer solution. The polymer solution was kept well stirred at a temperature of 45°C for about 4 h to completely dissolve the compound powder and then left to cool. Different concentrations of turmeric, walnut and henna, such as C_1 0.5 gm/L, C_2 0.25 gm/L and C_3 0.13 gm/L were added to the polymer gel matrix and kept well stirred for 1 h at room temperature. Solutions were prepared with different pH values (acidic pH_4 and alkaline pH_{10}) by using 1 Molar solution of sodium hydroxide (NaOH) and hydrochloric acid (HCl) respectively. Electrical conductivity of each dye solution was also determined. Thin films of 0.5 ml stock solution were made by pouring the dyed solution on a perfectly leveled glass plate and allowed to dry for 24 h at room temperature. The uniform and transparent dyed films were detached from the glass plate and sealed into small plastic bags and stored under laboratory conditions. The thickness of the dyed films was measured (Mai et al., 2008; Abdel-Fattah et al., 1996) and found to be 0.05 mm. The controlled sample of each dye film was kept un-irradiated (0 kGy). The prepared dye based radiochromic films were irradiated with Cs 137 Gamma rays source (Mark IV irradiator) at specific doses. Absorbed dose range for irradiation was selected and categorized into three levels, that is, low (0-1 kGy), intermediate (1-10 kGy) and high (10-100 kGy). The absorption spectra of un-irradiated and irradiated films were measured in the wavelength range of 200-800 nm (Shahid et al., 2013). λ_{max} for each dye was determined. The absorption spectra for each dye films were recorded at different doses (Abdel-Fattah et al., 1996; Ebraheem et al., 2002). Response curves were plotted between specific absorbance (A) at λ_{max} versus absorbed dose (D) for different concentrations (Nasef et al., 1995; Hussain et al., 2009; Shahid et al., 2012). Irradiated samples with maximum and minimum absorbance were subjected to XRD using X-ray diffractometer (Rigaku Model DMAX/11-A), AAS (Model Z-8200 Hitachi equipped with Zeeman Optical system), pH meter (no 8520 HANNA with ± 0.01 accuracy) and EC meter (LF 530 (WTW), USA standardized with ± 0.01 accuracy) were used in this study under ideal working conditions recommended for those instruments.

Irradiated samples with maximum and minimum absorbance were subjected to XRD under working conditions as given in Table 1. XRD analysis was performed on the basis of percentage crystallanity, crystallanity index (C.I), grain size (d), stress ($\boldsymbol{\eta}$), strain (ε) and modulus of elasticity (Y). Formulae used for calculations are as follows:

$$\% \text{ Crystallanity} = \frac{I_{max}}{I_{max}+I_{min}} \quad \ldots\ldots\ldots\ldots(1)$$

$$\text{Crystallanity index} = \frac{I_{max}}{I_n} \quad \ldots\ldots\ldots\ldots(2)$$

$$d = \frac{}{B} \quad \ldots\ldots\ldots\ldots(3)$$

$$\boldsymbol{\eta} = \frac{B\cos\theta\cdot}{\sin} \quad \ldots\ldots\ldots\ldots(4)$$

$$\varepsilon = \quad \ldots\ldots\ldots\ldots(5)$$

$$Y = \quad \ldots\ldots\ldots\ldots (6)$$

Explanation of the parameters used

Where A_o and A are the absorbance of the dye used before and after irradiation, $\boldsymbol{\varepsilon}$ is the molar extinction coefficient, λ is the wavelength used, B is the full width at half maxima, θ is the Bragg angle, I_{max} and I_{min} are the intensities of highest and lowest peaks of XRD pattern, Y is the modulus of elasticity and d is the particle size respectively.

Statistical analysis of data was also performed using SPSS version 13 program and ANOVA along with t-test and Chi square test to detect the decoloration effect due to gamma irradiation for different concentrations keeping in view the pH value and obvious influence was observed. Multiple comparisons were also carried out and

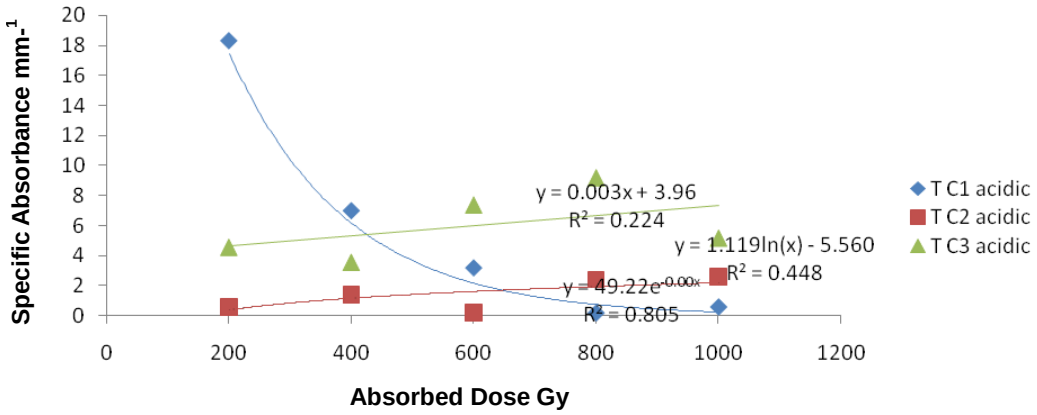

Figure 4. Graphical sketch for the effect of dose (0-1 kGy) on the specific absorbance (mm^{-1}) of T-PVA at $\lambda_{max=}$ 451 nm for different concentrations of T- acidic samples.

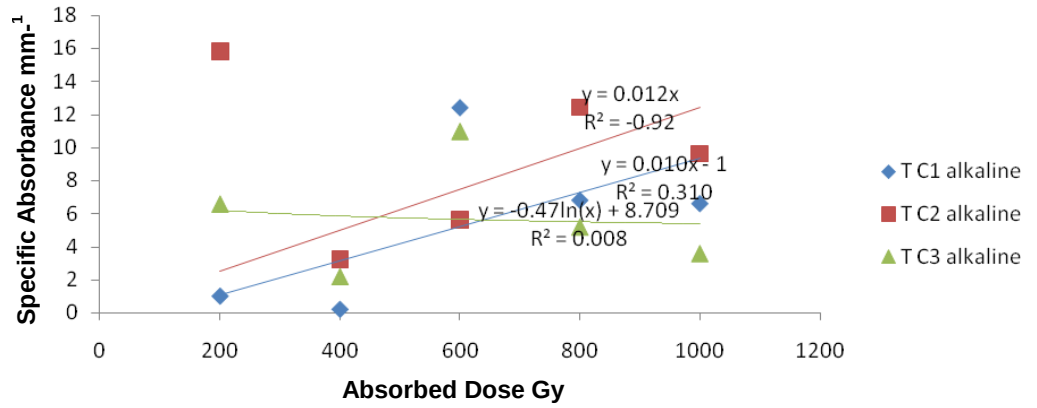

Figure 5. Graphical sketch for the effect of dose (0-1 kGy) on the specific absorbance (mm^{-1}) of T-PVA at $\lambda_{max=}$ 451 nm for different concentrations of T- alkaline samples.

the data were found extra stable for this study. To calculate statistical significance, p value ≤ 0.05 was considered significant.

RESULTS AND DISCUSSION

Due to irradiation, there was a visible color change for the dye films as shown in Figures 25-27 which show that some structural changes have occurred (Garcia et al., 2004; Parwate et al., 2007). This decoloration of the dye was studied in terms of change in specific absorbance of the dye films and the change in the structure of the dye was confirmed with the help of XRD analysis. Validity of Beer's law was confirmed in order to check the suitability of the selected dyes for dosimetric studies. The response curves of specific absorbance versus concentration showed approximate linear relationship between the specific absorbance of the film and concentration of the dye contained in the film as expected by the natural dyes which means that the dyes were best suited for dosimetric studies (Figures 4-21). Figures 4, 6, 8, 10, 12, 14, 16, 18 and 20 show the behavior of acidic samples, while Figures 5, 7, 9, 11, 13, 15, 17, 19 and 21 show behavior of alkaline samples of PVA films in low, intermediate and high dose range.

- Low dose range: Plot of specific absorbance versus dose showed that in low dose range, C_2 and C_3 of T-PVA, C_2 and C_3 of W-PVA acidic, C_1 and C_2 of T-PVA, and C_2 of W-PVA alkaline samples are best suited.
- Intermediate dose range: For the intermediate range, C_1 of T-PVA, C_3 of W-PVA acidic and C_3 of W-PVA, and C_1 and C_2 of H-PVA alkaline are useful.
- High dose range: For high dose range, all the three concentrations of T-PVA, C_2 of W-PVA acidic and C_1 of T-PVA, C_2 of W-PVA and C_2 and C_3 of H-PVA of alkaline samples worked best.

Behavior of radiation interaction with matter follows a

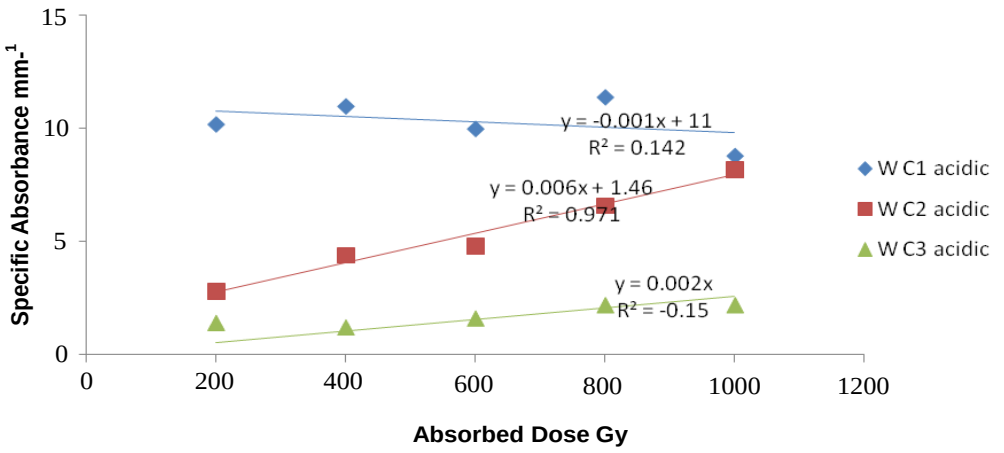

Figure 6. Graphical sketch for the effect of dose (0-1 kGy) on the specific absorbance (mm^{-1}) of W-PVA at $\lambda_{max=}$ 340 nm for different concentrations of W- acidic samples.

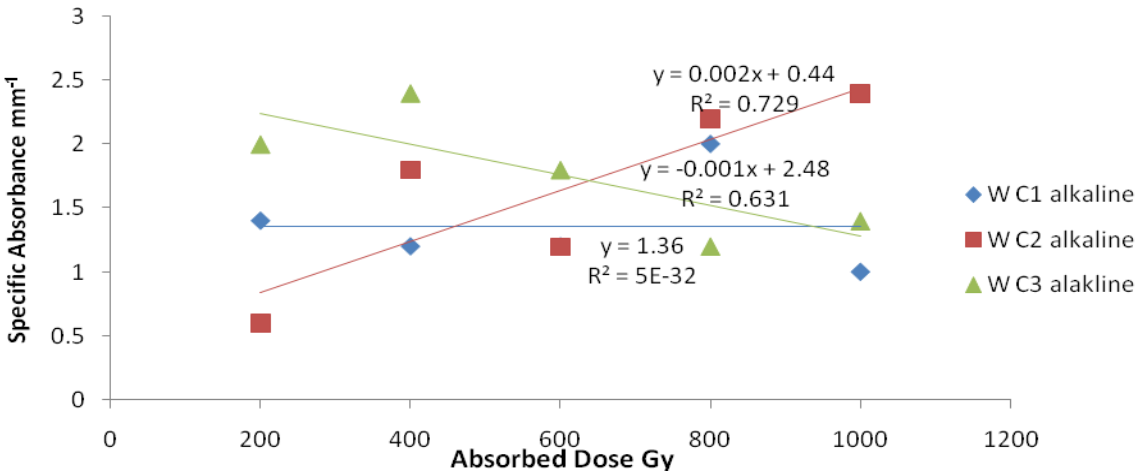

Figure 7. Graphical sketch for the effect of dose (0-1 kGy) on the specific absorbance (mm^{-1}) of W-PVA at $\lambda_{max=}$ 340 nm for different concentrations of W- alkaline samples.

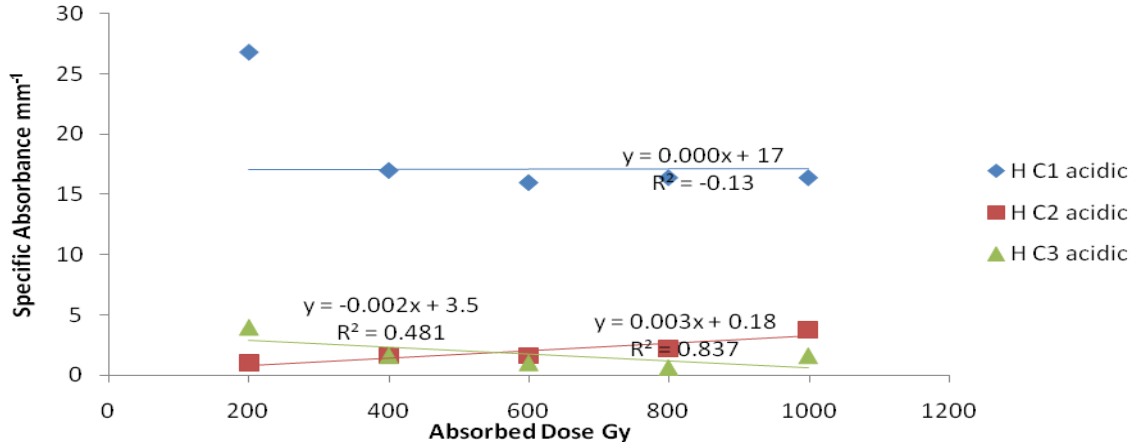

Figure 8. Graphical sketch for the effect of dose (0-1 kGy) on the specific absorbance (mm^{-1}) of H-PVA at $\lambda_{max=}$ 320 nm for different concentrations of H- acidic samples.

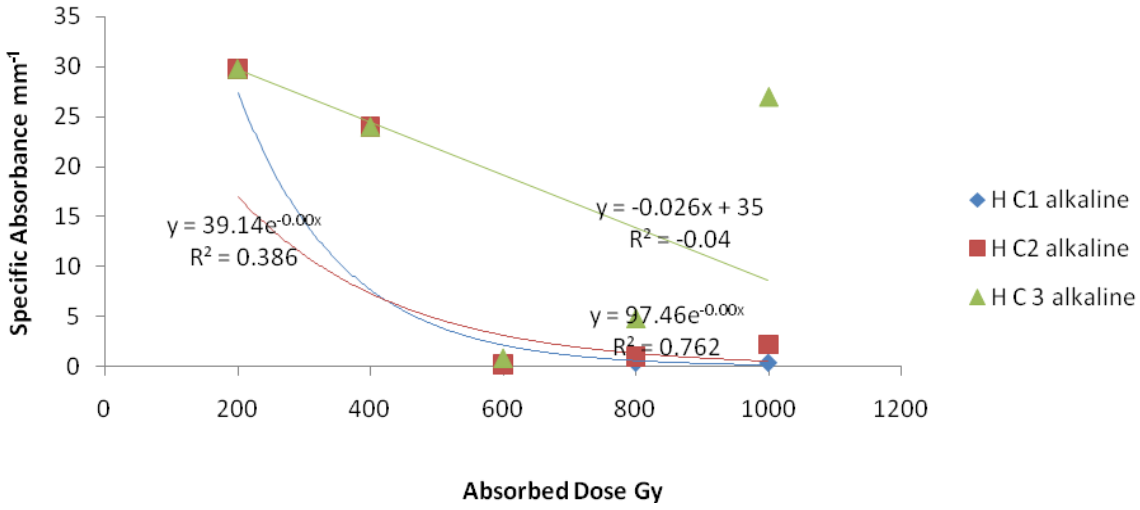

Figure 9. Graphical sketch for the effect of dose (0-1 kGy) on the specific absorbance (mm^{-1}) of H-PVA at $\lambda_{max=}$ 320 nm for different concentrations of H- alkaline samples.

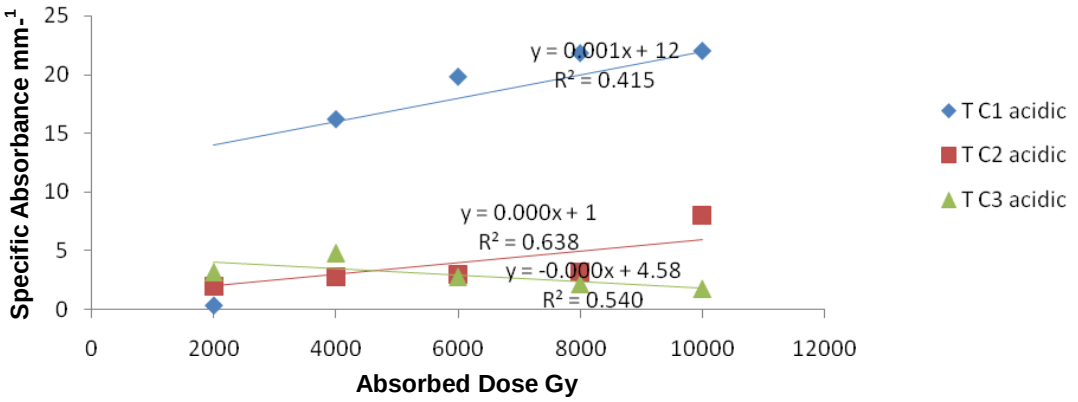

Figure 10. Graphical sketch for the effect of dose (1-10 kGy) on the specific absorbance (mm^{-1}) of T-PVA at $\lambda_{max=}$ 451 nm for different concentrations of T- acidic samples.

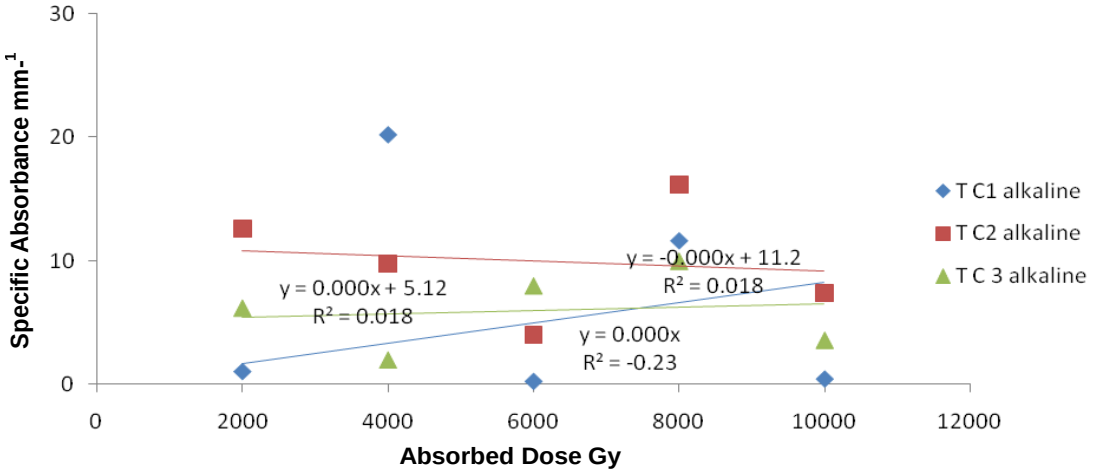

Figure 11. Graphical sketch for the effect of dose (1-10 kGy) on the specific absorbance (mm^{-1}) of T-PVA at $\lambda_{max=}$ 451 nm for different concentrations of T- alkaline samples.

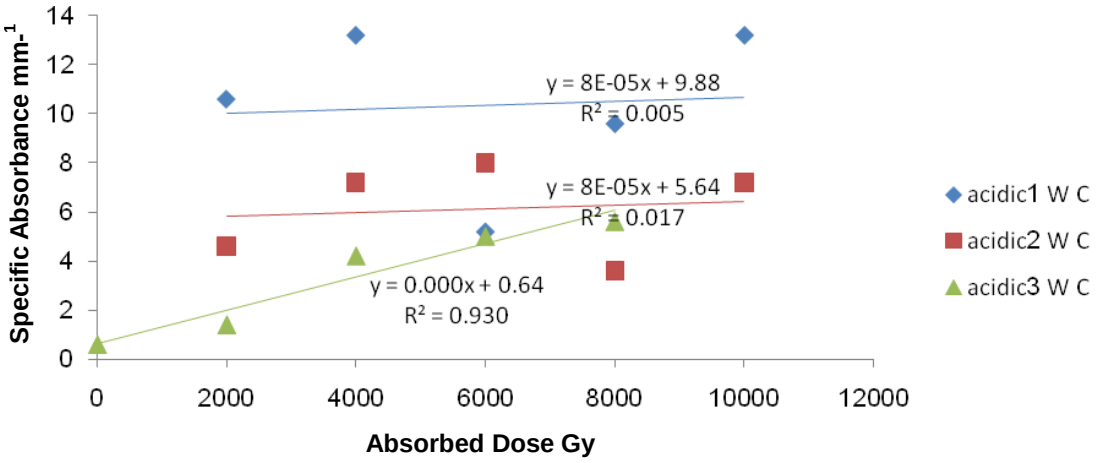

Figure 12. Graphical sketch for the effect of dose (1-10 kGy) on the specific absorbance (mm^{-1}) of W-PVA at $\lambda_{max=}$ 340 nm for different concentrations of W- acidic samples.

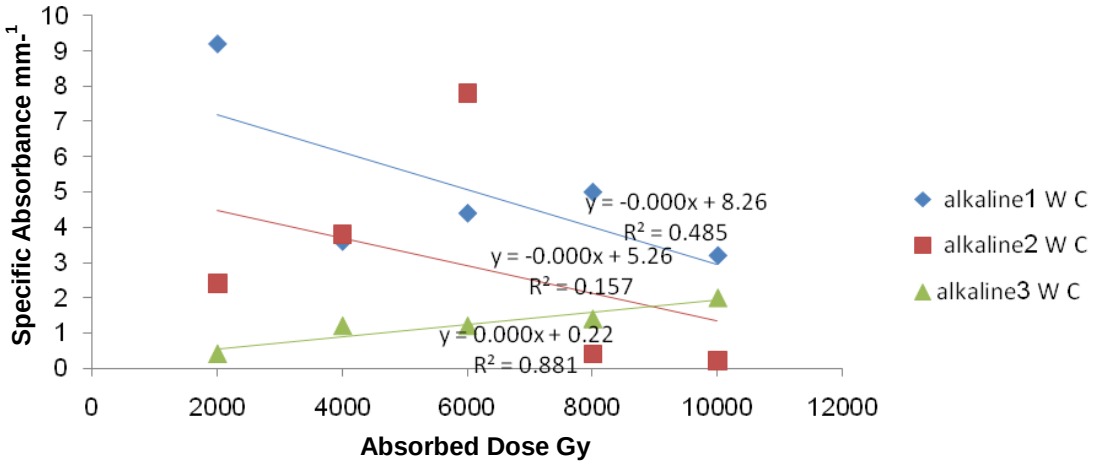

Figure 13. Graphical sketch for the effect of dose (1-10 kGy) on the specific absorbance (mm^{-1}) of W-PVA at $\lambda_{max=}$ 340 nm for different concentrations of W- alkaline samples.

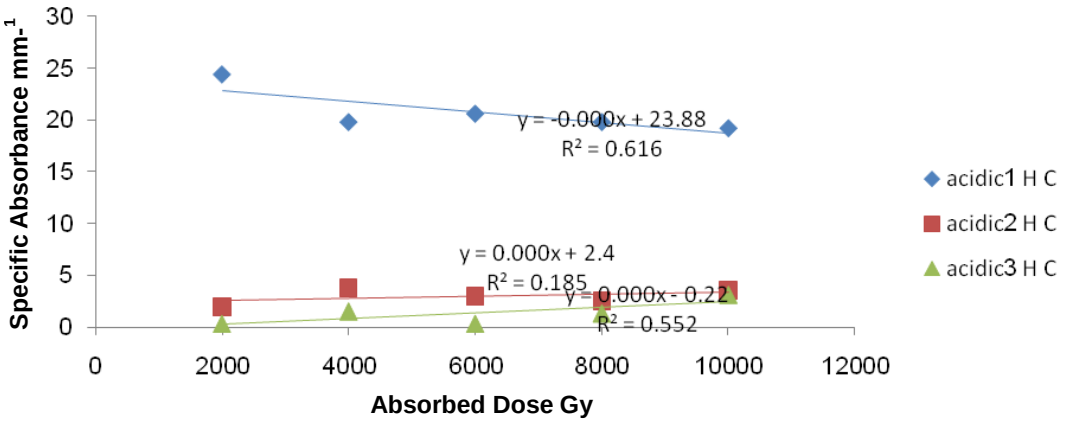

Figure 14. Graphical sketch for the effect of dose (1-10 kGy) on the specific absorbance (mm^{-1}) of H-PVA at $\lambda_{max=}$ 320 nm for different concentrations of H- acidic samples.

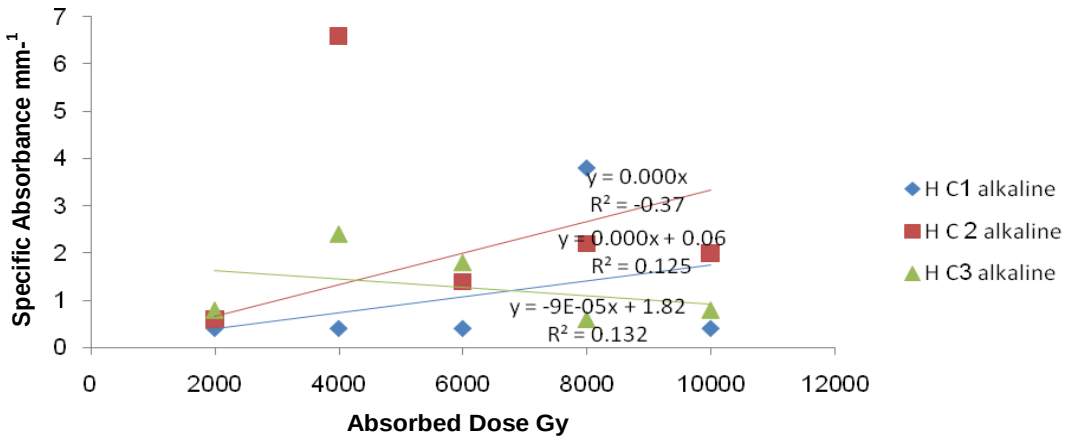

Figure 15. Graphical sketch for the effect of dose (1-10 kGy) on the specific absorbance (mm^{-1}) of H-PVA at $\lambda_{max=}$ 320 nm for different concentrations of H- alkaline samples.

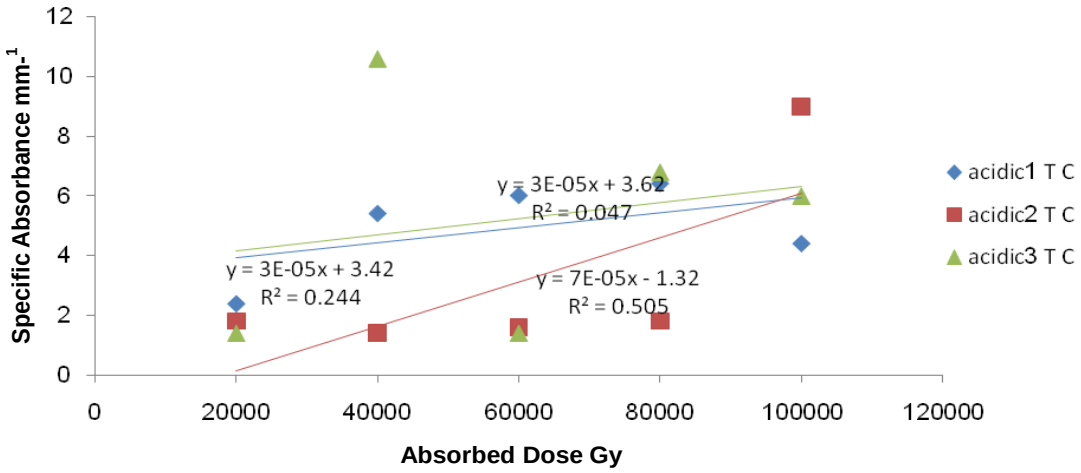

Figure 16. Graphical sketch for the effect of dose (10-100 kGy) on the specific absorbance (mm^{-1}) of T-PVA at $\lambda_{max=}$ 451 nm for different concentrations of T- acidic samples.

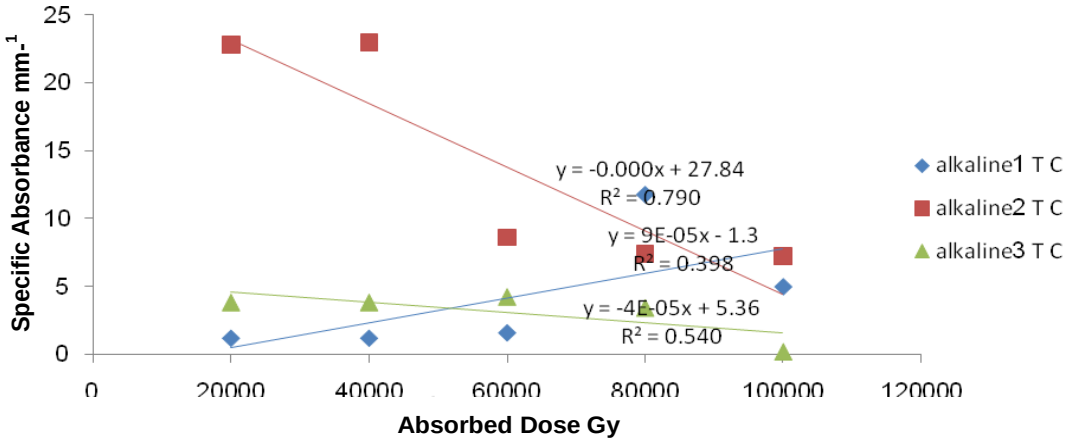

Figure 17. Graphical sketch for the effect of dose (10-100 kGy) on the specific absorbance (mm^{-1}) of T-PVA at $\lambda_{max=}$ 451 nm for different concentrations of T- alkaline samples.

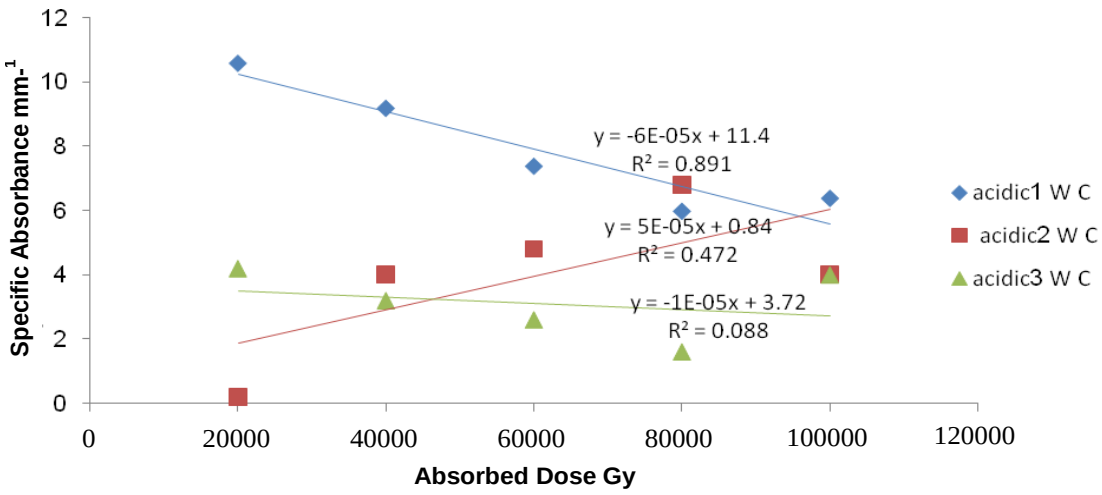

Figure 18. Graphical sketch for the effect of dose (10-100 kGy) on the specific absorbance (mm^{-1}) of W-PVA at $\lambda_{max=}$ 340 nm for different concentrations of W- acidic samples.

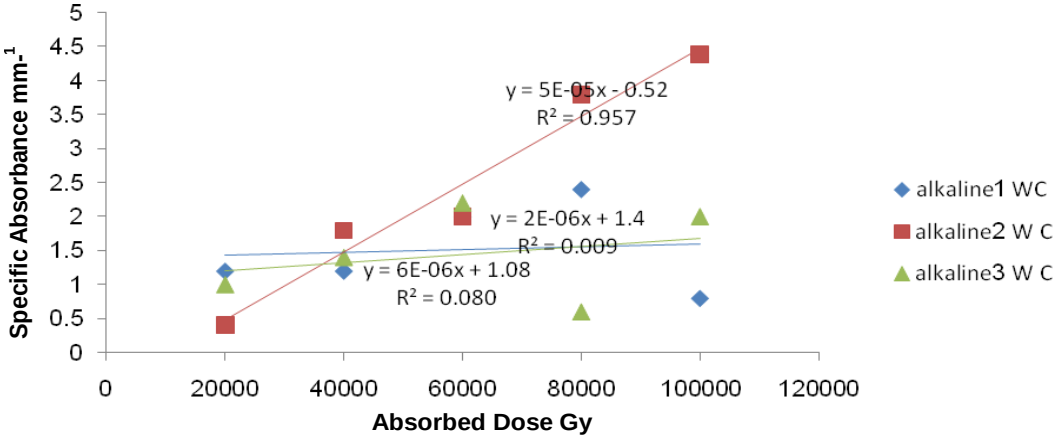

Figure 19. Graphical sketch for the effect of dose (10-100 kGy) on the specific absorbance (mm^{-1}) of W-PVA at $\lambda_{max=}$340 nm for different concentrations of W- alkaline samples.

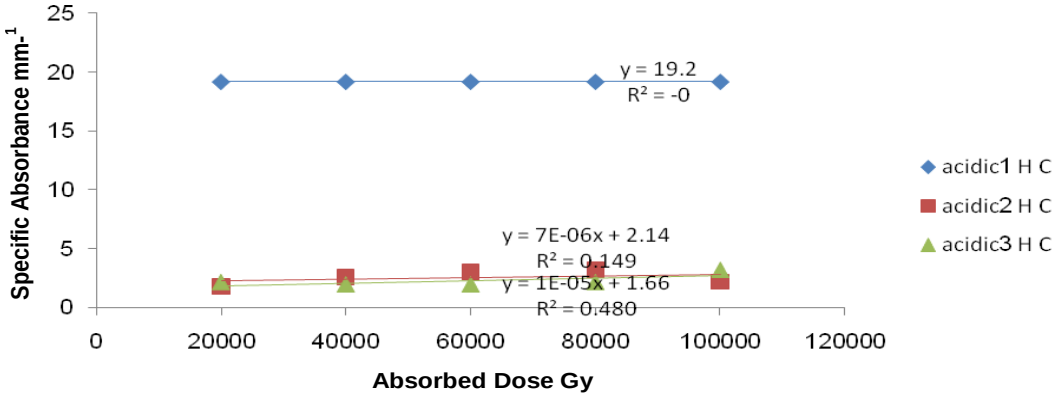

Figure 20. Graphical sketch for the effect of dose (10-100 kGy) on the specific absorbance (mm^{-1}) of H-PVA at $\lambda_{max=}$ 320 nm for different concentrations of H- acidic samples.

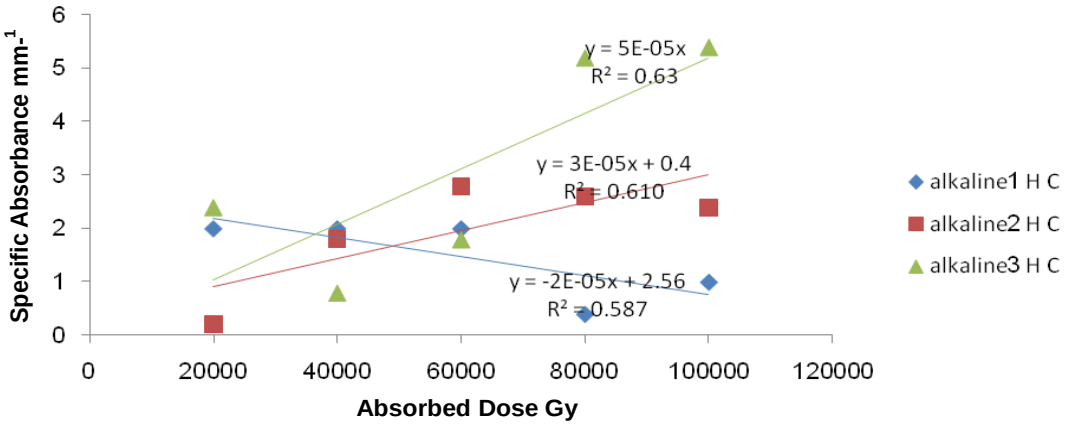

Figure 21. Graphical sketch for the effect of dose (10-100 kGy) on the specific absorbance (mm^{-1}) of H-PVA at $\lambda_{max=}$ 320 nm for different concentrations of H- alkaline samples.

linear model but no threshold due to artifacts formation disturbance during interaction and heat defects, which is the main problem in the chemical dosimetry. The model is represented by mathematical expression:

$$F(D) = (a_o + a_1D + a_2D^2 + \ldots\ldots + a_nD^n)x\ (e^{-b_1 D - b_2 D2})$$

where a_o = y intercept, and a_1 = linear coefficient or slope of the curve.

All others are determined through computer simulation for the most fit data. Linear model with threshold is only over simplification of data interpretation; the same assumption was used in this study and the linearity was approximated accordingly. Behavior of radiation interaction with matter follows a linear model but no threshold due to artifacts formation disturbance during interaction and heat defects, which is the main problem in the chemical dosimetry and can be explained mathematically on the basis of the following equations:

$$D_{med} = \frac{C_{med}\ \Delta T}{(1\text{-}h)}$$

D_{med} = dose measured
C_{med} = specific heat capacity of the medium.

and

h = heat defect.

This expression is further modified as:

$$D = dE_h/dm + dE_s/dm$$

where D = dose, dE_h/dm = energy appears as heat and dE_s/dm = energy absorbed or provided because of chemical change.

Dose response curve (H D curve) can be accessed on the basis of slope of the straight portion called Gamma (γ) of the film or γ-index. The criteria used for dose delivery acceptance in this study are γ≥1 rejected while γ≤1 accepted. In our case, R^2 serves the same purpose and the selection criteria was re-modified as R^2≥0.5 for acceptance due to random nature of the gamma interaction with the films (Vaijapurkar and Anuradha, 2010; Tachikaw et al., 2003; Samanta et al., 2009). This justification is completely in accordance with the theoretical model which can also be justified by our XRD results and physio-mechanical behavior of the dye.

It was observed that the samples with low pH values (acidic) are more sensitive to radiation. EC of each dye was measured in solution form before irradiation. It was found that EC for alkaline sample of each dye was greater than the acidic solution of the same dye ranging (880-1140 µS/cm) for turmeric, (330-1030 µS/cm) walnut and (291-1580 µS/cm) henna. It was also observed that EC increased with the concentration of the dye in solution (Riyadh et al., 2011). Radiation induced decoloration of dye based PVA films at the wavelength of maximum absorbance was investigated in the dose range of 0-100 kGy. Maximum degree of decoloration in the turmeric dye films was observed to be 94% in acidic form; in the walnut dye films, it was observed to be 51.5% in acidic form; and in henna dye films, it was observed to be 93.7% in alkaline form. Percentage decoloration for each concentration of the dye at specific doses is given in Tables 2 to 4.

According to Lambert's and Beer's law, the probability of absorbance in a medium is directly proportional to concentration of the absorbing atoms and thickness of the sample:

A = …… ……..(7)

The absorbance values at λ_{max} were obtained for three concentrations and molar extinction coefficient of irradiated and un-irradiated samples for each concentration was calculated using equation 7, keeping

Table 2. Percentage decoloration of T-PVA films.

D (Gy)	C1 Acidic	C2 Acidic	C3 Acidic	C1 Alkaline	C2 Alkaline	C3 Alkaline
200	54	26	21.9	2.9	57.2	39.2
400	20.5	6	17.1	0.58	11.6	13
600	94	0.8	35	36.2	19.6	65.4
800	0.58	10.4	43.8	19.8	44.9	30.9
1000	0.58	11.3	24.8	19.2	28.2	21.4
2000	1.17	8.6	15.2	2.9	45.6	36.9
4000	47.6	12.1	22.8	59	35.5	11.9
6000	58.2	13	13.3	0.58	14.4	47.6
8000	64	13.9	10.4	33.9	58.6	59.5
10000	5.8	34.7	8.5	1.16	26.8	21.4
20000	7	7.8	14.2	3.5	82.6	22.6
40000	15.8	6	50	3.5	83.3	22.6
60000	17	6.9	6.6	4.6	31.1	25
80000	18.8	7.8	32.3	34.5	26.8	20.2
100000	12.9	39	28.5	14.6	26	1.2

Table 3. Percentage decoloration of W-PVA films.

D (Gy)	C1 Acidic	C2 Acidic	C3 Acidic	C1 Alkaline	C2 Alkaline	C3 Alkaline
200	39.8	14.2	8.3	5.1	2.4	9.6
400	42.9	22.4	7.1	4.4	7.2	11.5
600	39	24.4	9.5	4.4	4.8	8.6
800	44.5	33.6	13	7.4	8.8	5.7
1000	38.2	41.8	13	3.7	5.6	6.7
2000	41.4	23.4	3.5	34	9.6	1.9
4000	51.5	36.7	8.3	13.3	15.3	5.7
6000	20.3	40.8	29.7	16.2	31.4	5.7
8000	37.5	18.3	29.7	18.5	1.6	6.7
10000	51.5	36.7	33.3	11.8	0.8	9.6
20000	41.4	1.02	25	4.4	1.6	4.8
40000	35.9	20.4	19	4.4	7.2	6.7
60000	28.9	24.4	15.4	7.4	8	10.5
80000	23.4	34.6	9.5	8.8	15.3	2.8
100000	25	20.4	23.8	2.9	17.7	9.6

path length constant in terms of thickness of the film, that is, l = 0.05 mm. Molar extinction coefficient at each dose for turmeric, walnut and henna dyes is given in Tables 5 to 7.

XRD pattern for C2 turmeric alkaline samples at 400 Gy and 40 kGy, C2 walnut acidic samples at 0 Gy and 10 kGy, and C3 henna alkaline samples at 1 kGy and 40 kGy, having maximum and minimum absorbance are given in Figures 22 to 24.

XRD analysis

The counter reading of the highest peak intensity near 23° represents crystalline material, while the peak near 16°, which is the lowest intensity (halo-pattern), corresponds to the amorphous material in the PVA films.

As far as the degree of Crystallanity and Crystallanity index is concerned with respect to maximum and minimum absorbance, turmeric and henna showed slight variations but re-adjustable properties while walnut showed complete stability showing minimum structure damage and lattice dislocations confirmed through mechanical properties and hence can safely be used as dosimeters. Physio-mechanical behavior of the dye films is discussed in Table 8.

DISCUSSION

In this study, the suitability of natural dyes (turmeric, walnut and henna) for secondary dosimeter was checked

Table 4. Percentage decoloration of H-PVA films.

D (Gy)	C1 Acidic	C2 Acidic	C3 Acidic	C1 Alkaline	C2 Alkaline	C3 Alkaline
200	84.8	3.3	16.6	1.2	3.4	4.1
400	53.7	5.3	6.6	1.2	13.7	2.1
600	50.6	5.3	4.2	1.2	0.68	2.7
800	51.8	7.3	2.5	1.2	3.4	16.6
1000	51.8	12.7	6.6	1.2	7.5	93.7
2000	77.2	6.7	1.6	1.2	2	2.7
4000	62.6	12.7	6.6	1.2	22.7	8.3
6000	65.1	10	1.6	1.2	4.8	6.2
8000	62.6	8.7	5.8	11.7	7.5	2
10000	64.7	12	13.3	1.2	6.8	2.7
20000	60.7	6	9.1	6.1	0.68	8.3
40000	60.7	8.7	16.6	6.1	6.2	46.7
60000	60.7	10	8.3	6.1	9.6	6.2
80000	60.7	10.7	9.1	6.1	8.9	18
100000	60.7	7.3	13.3	3	8.2	18.7

Table 5. Molar extinction coefficients [$(g/L)^{-1}mm^{-1}$] for T-PVA.

Dose (gy)	C1 Acidic	C2 Acidic	C3 Acidic	C1 Alkaline	C2 Alkaline	C3 Alkaline
0	68	92	161.5	68.4	110.4	129.2
200	31.5	89.6	126.1	66.4	47.2	78.46
400	54	86.4	133.8	68	97.6	112.3
600	61.6	91.2	104.6	43.6	88.8	44.6
800	67.6	82.4	90.76	54.8	60.87	89.2
1000	66.8	81.6	121.5	55.2	79.2	101.5
2000	67.2	84	136.9	66.4	60	81.5
4000	35.6	80.8	124.6	28	71.2	113.8
6000	28.4	80	140	68	94.4	67.6
8000	24.4	79.2	144.6	45.2	45.6	52.3
10000	24	60	147.6	67.6	80.8	101.5
20000	63.2	84.8	150.7	66	19.2	100
40000	5702	86.4	80	66	18.4	100
60000	56	85.6	150.7	65.2	76	96.9
80000	55.2	84.8	109.2	44.8	80.8	103
100000	59.2	56	115.3	58.4	81.6	127.6

for different doses along with its acidic and alkaline nature when irradiated with Gamma source for different doses. The behavior of acidic and alkaline samples of the PVA film was checked after low, intermediate and high gamma dose irradiation for C_1, C_2 and C_3 concentrations and it was observed that in low dose range, C_2 and C_3 of T-PVA, C_2 and C_3 of W-PVA acidic, C_1 and C_2 of T-PVA, and C_2 of W-PVA alkaline samples are best suited. For intermediate range, C_1 of T-PVA, C_3 of W-PVA acidic, C_3 of W-PVA, and C_1 and C_2 of H-PVA alkaline are useful. For high dose range, all the three concentrations of T-PVA, C_2 of W-PVA acidic, C_1 of T-PVA, C_2 of W-PVA, and C_2 and C_3 of H-PVA of alkaline samples worked best.

Wide margin of pH values and wide variation in EC confirmed the radiolysis and random fashioned behavior of the dye confirming the gamma rays interaction with the dye making dose delivery into the dye structure. XRD studies and physio- mechanical properties also favor our findings. The detailed discussion of our experimental findings is as follows.

It was observed that the samples with low pH values (acidic) are more sensitive to radiation. EC of each dye was measured in solution form before irradiation. It was found that EC for alkaline sample of each dye was

Table 6. Molar extinction coefficients [(g/L)-1mm-1] for W-PVA.

Dose	C1 Acidic	C2 Acidic	C3 Acidic	C1 Alkaline	C2 Alkaline	C3 Alkaline
0	51.2	78.4	129.2	54	99.2	160
200	30.8	67.2	118.6	51.2	96.8	144.6
400	29.2	60.8	120	51.6	92	141.5
600	31.2	59.2	116.9	51.6	94.4	146.1
800	28.4	48	112.3	50	90.4	150.7
1000	31.6	45.6	112.3	52	89.6	149.2
2000	30	68	124.6	35.6	89.6	156.9
4000	24.8	49.6	118.4	46.8	84	150.7
6000	40.8	46.4	96.9	45.2	68	150.7
8000	32	64	90.7	44	97.6	149.2
10000	24.8	49.6	86.1	47.6	98.4	144.6
20000	30	77.6	96.9	51.6	97.6	152.3
40000	32.8	62.4	104.6	51.6	92	149.2
60000	36.4	59.2	109.2	50	91.2	143
80000	39.2	51.2	116.9	49.2	84	155.3
100000	38.4	62.4	98.46	52.4	81.6	144.6

Table 7. Molar extinction coefficients [$(g/L)^{-1}mm^{-1}$] for H-PVA.

Dose	C1 Acidic	C2 Acidic	C3 Acidic	C1 Alkaline	C2 Alkaline	C3 Alkaline
0	63.2	119.2	184.6	64.8	116	221.5
200	9.6	115.2	153.8	64	112	212.3
400	29.2	112.8	172.3	64	100	216.9
600	31.2	112.8	176.9	64	115.2	215.3
800	30.4	110.4	180	64	112	184.6
1000	30.4	104	172.3	64	107.2	13.8
2000	14.4	111.2	181.5	64	113.6	215.3
4000	23.6	104	172.3	64	89.6	203
6000	22	107.2	181.5	64	110.4	207.6
8000	23.6	108.8	173.8	57.2	107.2	216.9
10000	24.8	104.8	160	64	108	215.3
20000	24.8	112	167.6	60.8	115.2	203
40000	24.8	108.8	153.8	60.8	108.8	215.3
60000	24.8	107.2	169.2	60.8	104.8	207.6
80000	24.8	106.4	167.6	64	105.6	181.5
100000	24.8	110.4	160	62.8	104	180

greater than the acidic solution of the same dye ranging from 880-1140 µS/cm for turmeric, 330-1030 µS/cm for walnut and 291-1580 µS/cm for henna. It was also observed that EC increased with the concentration of the dye in solution (Riyadh et al., 2011). Radiation induced decoloration of PVA films at the wavelength of maximum absorbance was investigated in the dose range of 0-100 kGy. Maximum degree of decoloration in the turmeric dye was observed to be 94% in acidic, for walnut it was 51.5% in acidic and for henna dye it was 93.7% in alkaline form.

PVA films possessed both crystalline and amorphous phases. Crystallanity is co-related to the strength of the film, may be as a result of reinforcement in the structure. Crystallanity index gives a quantitative measure of the orientation of the crystals in the sample, its lower value means disorientation of the lattice, without disturbing the PVA film form and converse. From XRD pattern, it is also evident that the dye structure is a mixture of different kinds of minerals comprising organic and inorganic components, superimposed upon each other, making their structures heterogeneous and behaviors complex.

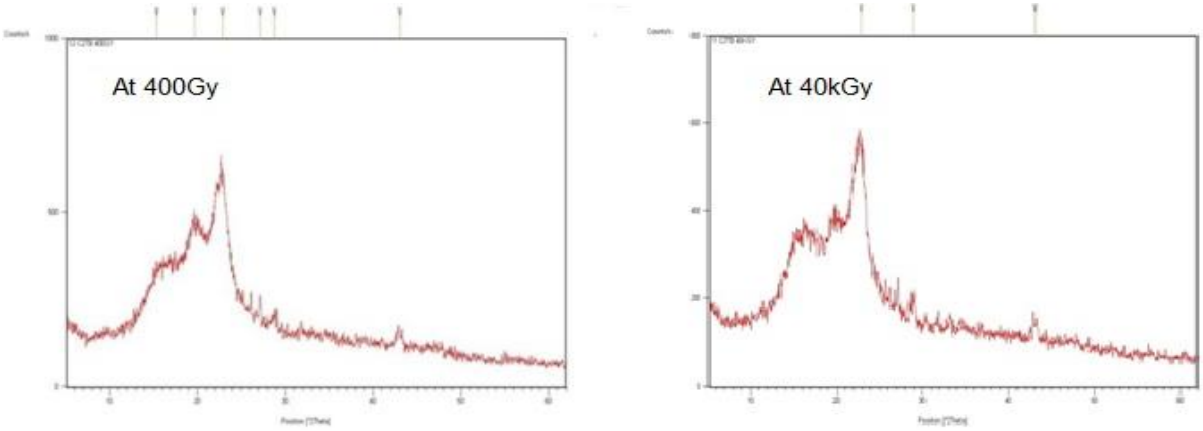

Figure 22. XRD pattern of C2T alkaline at 400 Gy and 40 kGy.

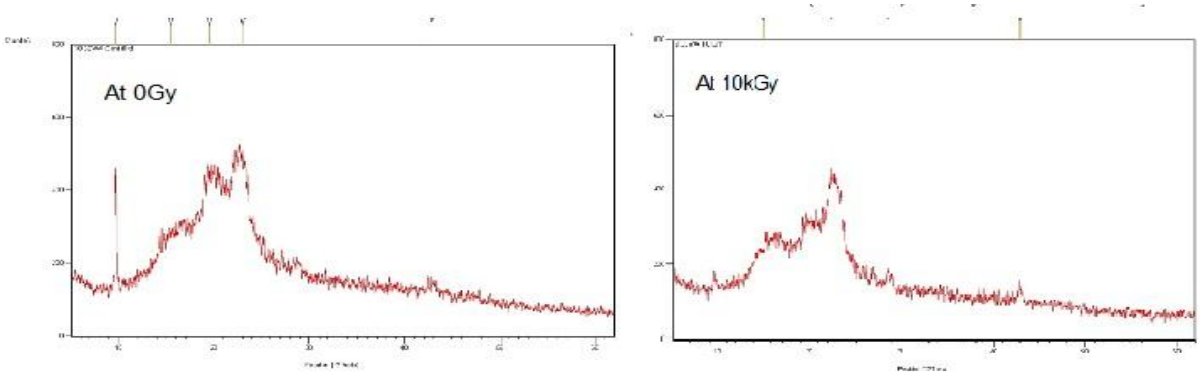

Figure 23. XRD pattern of C2W acidic at 0 Gy and 10 kGy.

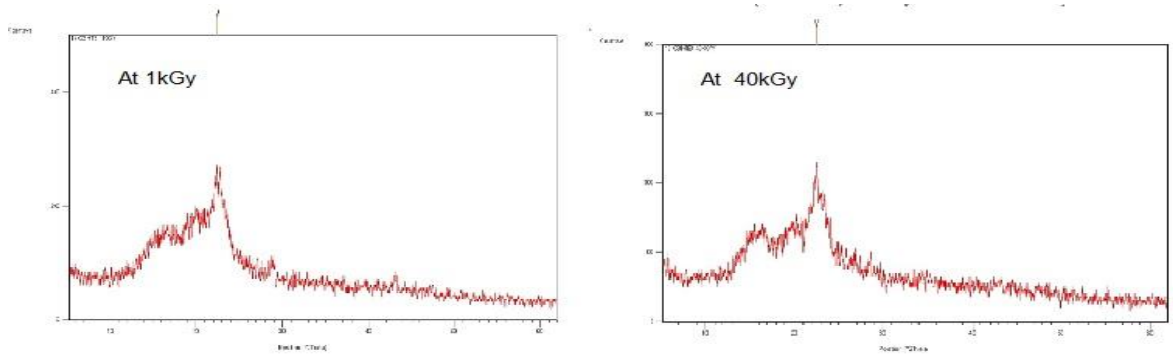

Figure 24. XRD pattern of C3H alkaline at 1 kGy and 40 kGy.

Wide margin fixed for pH values (4-10) and wide variations in EC, that is, between 880 and 1140 µS/cm for turmeric, 330 and 1030 µS/cm for walnut, and 291 and 1580 µS/cm for henna predicts that the process of radiolysis took place when PVA films were irradiated with Gamma source, but in a random fashion which is the main feature of the radiolysis, hence the use of films as dye dosimeters cannot be ruled out. As far as the degree of Crystallanity and Crystallanity index is concerned with respect to maximum and minimum absorbance, turmeric and henna showed slight variations but re-adjustable pattern, but walnut showed complete stability upon

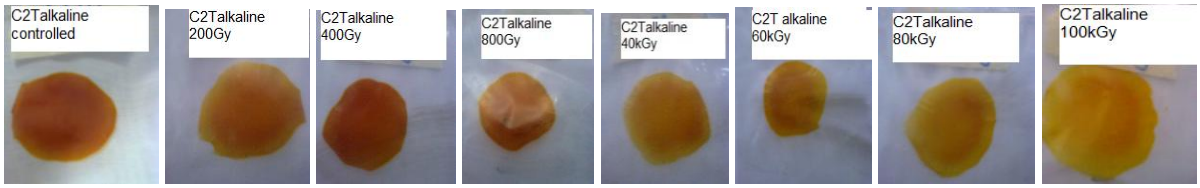

Figure 25. Photographs of Turmeric C2 alkaline sample films showing decoloration at different doses.

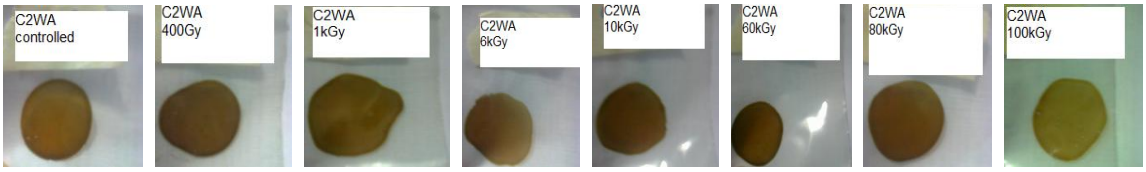

Figure 26. Photographs of Walnut C2 acidic sample films showing decoloration at different doses.

irradiation showing minimum structure damage and lattice dislocations confirmed through mechanical properties and hence can safely be used as dosimeters. The main feature of radiolysis is the creation of OH^- ions. As OH^- active ions contribute much in dye structure bonds, breakage in dye is attached with internal structure damage and hence it serves as color centers within the lattice of the dye. A higher value of EC in case of turmeric shows the possibility of large number of charge carriers within the lattice. From the molecular structure of turmeric shown in Figure 1, it is evident that greater amount of OH^- ions can be generated so the color degradation is higher in the case of turmeric. So, the percentage decoloration decreased with absorbed dose linearly in the low dose range, that is, at 200 Gy, %age decoloration is 57.2%, but at 400 Gy, it is 11.6%. This decrease in the %age decoloration means the enhancement of color and the increase in %age crystallanity which can be seen in the photographs of T-PVA films (Figure 25). However, for 200 and 400 Gy, there is an enhancement of color. From 400-800 Gy, the value of %age decoloration increased. From 400 Gy-40 kGy, %age decoloration increased almost linearly and reached its maximum value, that is, 83.3%. We have selected the samples having maximum and minimum values of %age decoloration to study the overall behavior of the dye and for these samples the molar extinction coefficient changed with absorbed dose in accordance with the increase in specific absorbance. %age crystallanity and C.I also favor our findings, which means that the process of radiolysis have taken place. Study of mechanical properties shows that there is a decrease in particle size due to the increase in compressive stresses within the crystal lattice. The value of Modulus of Elasticity increased for turmeric dye but remained within the elastic limits. It means that turmeric has a stable crystalline structure. If the structure is damaged due to the absorption of radiation, it recovers the symmetry immediately. Moreover, the OH^- ions serve as color centers within the lattice. The breakage of bonds and the formation of new bond or shifting of color centers and their re-establishment is mainly the reason of this randomness in the behavior of the dye (Paul et al., 2010; Patel and Dixit, 2012).

In the case of walnut dye, specific absorbance decreased with increasing dose in the low dose range resulting to a linear increase in percentage decoloration. Molar extinction coefficient also increased due to decrease in specific absorbance. From Figure 26, it is clear that decoloration increased up to 1 kGy. After 1 kGy, it decreased sharply and then increased linearly in the intermediate dose range up to 10 kGy. Molar extinction coefficient decreased to its lowest value which shows that maximum absorption of radiation has occurred. To study the effect of absorbed dose on the structure of the dye, samples were subjected to XRD analysis. For XRD analysis, the control samples were selected before the sample having the minimum value of %age decoloration was selected. The %age decoloration at 10 kGy was 36.7% which is the sample of interest but enhancement of color was observed at this dose (Figure 26). The percentage crystallanity and crystallanity index for controlled and irradiated sample at 10 kGy dose showed that both percentage crystallanity and crystallanity index increased but the particle size remained almost the same (Table 8). Modulus of Elasticity changed its value from negative to positive. It means that the sample having elastic properties, after absorbing radiation when it rearranged itself, turns into plastic material which is highly symmetric and this is the reason of increase in percentage crystallanity and crystallanity index. More refined and transparent films were observed in terms of color which can also be seen from Figure 26. Hardness of the films was increased due to irradiation which confirms the change in mechanical properties of the films.

Table 8. Physio-mechanical behavior of selected samples of dyes (Turmeric, Walnut and Henna) at specific doses.

Dye	Turmeric		Walnut		Henna	
Dose	**400 Gy**	**40 kGy**	**0 Gy**	**10 kGy**	**1 kGy**	**40 kGy**
Absorbance	1.22	0.23	0.98	0.62	0.09	1.4
%age decoloration	11.6	83.3	0	36.7	93.7	46.7
Molar extinction coefficient $[(g/L)^{-1}mm^{-1}]$	97.6	18.4	78.4	49.6	13.8	215.3
%age crystallanity	65.8	60.3	59.5	64.5	59.8	62.5
Crystallanity index	0.48	0.34	0.32	0.45	0.32	0.40
Particle size (nm)	4.132	3.709	4.132	4.136	3.709	4.134
Stress (Nm^{-2})	-5.498×10^{-6}	-5.029×10^{-6}	-5.498×10^{-6}	1.006×10^{-5}	-5.029×10^{-6}	2.822×10^{-6}
Strain	0.043	0.0478	0.043	0.042	0.0478	0.043
Modulus of elasticity (Nm^{-2})	-1.28×10^{-4}	-1.05×10^{-4}	-1.28×10^{-4}	2.39×10^{-6}	-1.05×10^{-4}	6.6×10^{-5}

Figure 27. Photographs of Henna C3 alkaline sample films showing decoloration at different doses.

Percentage decoloration in the case of walnut has a much lower value than turmeric. The reason may be lower values of EC in the case of walnut. Due to radiolysis, less number of OH^- ions is generated. As OH^- ions are responsible for decoloration, so maximum of 51.5% decoloration was observed (Soutsas, 2010).

For henna C3 alkaline, the behavior of the dye was entirely different. Specific absorbance decreased linearly with increasing absorbed dose in the low and intermediate dose range but increased in high dose range. Percentage decoloration increased linearly in the low dose range and reached its maximum value of 93.7% then changed abruptly in the intermediate dose range. At 6 kGy, it decreased to 6.2% which is shown in Figure 27 that enhancement of color was observed at this dose. In the high dose range, it reaches a maximum value of 46.7% at 40 kGy. Sample selection was made on the basis of maximum decoloration in low dose range and the sample having maximum decoloration in the high dose range. The change in optical properties is such that specific absorbance increased while percentage decoloration and molar extinction coefficient decreased. The comparison of structural properties was made on the basis of percentage crystallanity and crystallanity index and change in mechanical properties was studied using XRD analysis. It was observed that percentage crystallanity and crystallanity index increased. Particle size also increased. Elastic modulus changed from negative to positive which shows that elastic material turns to plastic material. The mechanical behavior of both walnut and henna dyes is almost similar. The reason for this symmetric and similar behavior is that they have similar molecular formula but different molecular structure. Moreover much difference in percentage decoloration is due to a large difference in EC values (330 µS/cm for walnut in acidic form and 1580 µS/cm for henna in alkaline solution). As observed in this study that OH^- ions are serving as color centers within the lattice, formation of OH^- ions as a result of radiolysis are responsible for higher decoloration in the case of henna as compared to walnut (Khanmohammadi and Erfantalab, 2012; Guimaraes et al., 2012).

The physics behind the slight disagreement is that in this study bulk behavior of gamma interaction with films for specific energy ranges has been studied and probabilistic nature of quantum mechanical phenomenon like photoelectric effect, compton effect and pair production has been over simplified. The actual case of disagreement is that the polymerization after irradiation causes a post exposure density growth and emergence of automated darkening shadows resulting in an increase in optical density and consequently producing errors and finally abnormality in their behavior. To overcome this discrepancy, two irradiation plans were prepared to simulate low dose and high dose conditions, so that the signal to noise ratio becomes smaller and smaller and can be ignored, though optimization of this condition needs more rigorous research (Samanta et al., 2010;

Vajapurkar, 2010).

The results presented in this work are related only to the part of our mega project “chemical dosimetry” which includes also the topographical and morphological structure. Studies using SEM and TEM along with crystal dislocations using AFM and correlation of these results with film discoloration are in progress; it is hoped that after completion of the project we will be in a better position to comment on the causes of non-linear behavior of the PVA films during dose delivery and partial disagreement of our results with the published literature (Tiwari et al., 2010; Vaijapurkar, 2008).

Conclusion

λ_{max} for T=451 nm, W=340 nm and H=320 nm was recorded. Response curve for specific absorbance versus concentration showed linear behavior for each dye. Maximum degree of decoloration in the turmeric, walnut and henna dye films was observed to be 94, 51.5 and 93.7% respectively. XRD analysis was performed and % crystallanity and crystallanity index was calculated. On the basis of these calculations, it was observed that for turmeric, %age crystallanity as well as crystallanity index decreased due to irradiation which means some crystal dislocations have occurred which is the cause of decoloration of the dye. While for W and H, % crystallanity and crystallanity index increased.

Study of mechanical properties of dye films confirmed the results based on spectrophotometry and % crystallanity. It was further concluded that radiolysis has been revealed to be a capable alternative for hazardous contamination annihilation and has been confirmed for a large validity of pollutants. In this way, the induced radiation techniques help us to solve not only environmental cum health hazard problems but also damage measurements, and provide us an indication to adopt protective measures. XRD study also revealed that Gamma induced degradation is the most efficient, extra safe and environment friendly method for dye dosimetery investigation. The important conclusions drawn from this study are that interaction of gamma rays with PVA films is a complex phenomenon and the behavior of the films is not ideally elastic as was expected. At certain regions, especially high dose and low dose gradient regions, they showed mix behavior, that is, elastic cum plastic. This study also confirms the limitations of natural dyes like difficulty in selecting standard recipe for the use of dyes, lack of precise relevant technical knowledge about dye extraction and their fugitive nature. However, XRD analysis confirmed the said findings (Samanta et al., 2009).

LIMITATIONS

- pH of the solution is the major parameter which affects the specific absorbance of the film, so its value can vary to check the dose behavior on the film for dye dosimetry.
- pH and EC are related to free charge carriers available within the crystal lattice. As gamma rays which interact with the crystalline dye electron-hole pairs are created, so both of the above stated parameters will be changed. Change in pH and EC can be the parameter of interest in order to understand the behavior of the dye.

FUTURE RECOMMENDATIONS

- More detailed study of collective behavior of the dye can be made on the basis of change in morphology and topography using SEM and TEM. No doubt, the dosimetry is a quantum mechanical/nuclear phenomenon especially in the case of chemical dosimetry, but microscopical changes coupled with macroscopical changes show bulk behavior which is only possible through the study of morphology and topography of the films before and after irradiation.
- Chemical changes that have occurred in the dye structure due to gamma ray interaction can be analyzed by FTIR.

ACKNOWLEDGMENTS

Special thanks to Prof. Dr. Shaukat Ali, Department of Chemistry, UAF for providing us artificial dyes; and Professor Dr. Shaukat Ali Shahid, Department of Physics, UAF for providing us lab facilities for spectrophotometric analysis. More so, Dr. Naseem Akhtar, DCS, NIAB and Director NIAB Faisalabad for providing us with Gamma irradiation facilities available in their prestigious institution along with their technical and non-technical teams to accomplish this task within the shortest possible time will always be remembered.

REFERENCES

Abdel-Fattah AA, Ebraheem S, El-Kelany M, Abdel-Rehim (1996). High dose film dosimeters based on Bromophenol Blue or Xylenol Orange dyed polyvinyl alcohol. Appl. Radiat. Isot., 47:345-350.

Ali S, Umbreen S, Hussain T, Nawaz R (2008). Dyeing Properties of Natural Dyes Extracted from Turmeric and their Comparison with Reactive Dyeing. RJTA, Vol. 12(4). 1-6.

Al-Zahrany AA, Rabaeh KA, Basfer AA (2011). Radiation induced color bleaching of methyl red in polyvinyl butyral film dosimeter. Radiat. Phys. Chem., 80: 1263-1267.

Baha A, Abdul Halim NH, Zainal Abidin NA (2011). Influence of sunlight on absorption spectra of Rhizophora Apiculata dye solution. IEEE colloquium on humanities, science and engineering research (CHUSER 2011).

Baha A, Hashini NHM, Abdul Halim NH, Zainal Abidin NA, Me R, Hasan S (2012). Degradation of Rhizophora Apiculata dye solution under sunlight exposure, IEEE Business, Engineering and Industrial Applications Colloquium (BEIAC).

Basfar AA, Khalid AR, Akram AM, Rashed IM (2011).

Dosimetric characterization of nitro-blue tetrazolium polyvinyl butyral films for radiation processing. Radiat. Phys. Chem., 80: 763-766.

Blaskov V, Stambolova I, Shipochka M, Vassilev S, Kaneva N, Loukanov A (2011). Decoloration of Reactive Black 5 Dye on TiO2 Hybrid films Deposited by Sol-Gel Method, Scientific papers, Vol: 38, Book 5, 2011- Chemistry.

Buttery RG, Light DM, Nam Y, Merrill GB, Roitman JN (2000). Volatile components of green walnut husks. J. Agric Food Chem., 48 (7), 2858-2861.

Calogero G, Marco GD (2008). “Red Sicilian orange and purple eggplant fruits as natural sensitizers for dye-sensitized solar cells”, Sol. Energ. Mat. Sol. C 92 1341-1346.

Chen YP, Liu SY, Yu HQ, Yin H, Li QR (2008). Radiation induced degradation of Methyl Orange in aqueous solutions, Chemosphere, 72: 532–536.

Ebraheem S, Eid S, Kovacs A (2002). A new dyed polyvinyl (vinyl alcohol) film for high dose application, Radiat. Phys. Chem., 63: 807-811.

Garcia R, Harris A, Winters M, Howarda B, Mellora P, Patila D, Meinera J (2004). Absorbed dose measurement in low temperature samples comparative methods using simulated material, Radiat. Phys. Chem., 71:349–352.

Guimaraes JR, Maniero MG, de-Araujo RN (2012). A comparative study on the degradation of RB-19 dye in an aqueous medium by advanced oxidation processes, Int. J. Enveron. Manage., vol. 110, pp: 33- 39.

Hussain MY, Islam-ud-Din, Hussain T, Akhtar N, Ali S, Inam-ul-Haq (Provide Initials) (2009). Response of Sandal Fix Red C4BLN dye solutions using Co^{60} gamma-Radiation source at intermediate doses, Pak. J. Agric. Sci., 46(3):224-227.

Khanmohammadi H, Erfantalab M (2012). New 1, 2,4-triazole-based azo- azomethine dyes. Part I: Synthesis, characterization and spectroscopic studies. Spectrochimica Acta Part A: Mol. and Biomol. Spect. 86:39-43.

Mai HH, Solomon HM, Taguchi M. Kojima T (2008). Polyvinyl butyral films containing leuco-malachite green as a low-dose dosimeter, Radiat. Phys. and Chem., 77:457-462.

Mehta K, Girzikowsky R (1995). Reference dosimeter system of the IAEA, Radiat Phys Chem, 46:4-6.

Nasef B, El-Assy, Yun-dong C, Walker ML, Sheikhly MA, Mclaughlin WL (1995). Anionic triphenylmethane dye solutions for low-dose food irradiation dosimetry, Radiat. Phys. Chem, 46:1189-1197.

Parwate DV, Sarma ID, Batra R (2007). Preliminary feasibility study of congo red dye as a secondary dosimeter, Rad Meas 42(9):1527-1529.

Patel HM, Dixit BC (2012). Synthesis, characterization and dyeing assessment of novel acid azo dyes and mordent acid azo dyes based on 2-hydroxy-4-methoxybenzophenone-5-sulfonic acid on wool and silk fabrics. ǁ. J. Saudi Chem. Soc., In press.

Paul J, Naik DB, Sabharwal S (2010). High energy induced decoloration and mineralization of Reactive Red 120 dye in aqueous solution: A steady state and pulse radiolysis study. ǁ Radiat. Phys. Chem., vol. 79, pp: 770- 776.

Riyadh Ch, Ghufran AH, Shabeeb M, Hammouti B (2011). Characterization of table sugar dosimeter for gamma-radiation dosimetry, Der Pharma Chemica, 3(6): 182-188.

Sachin K, Kapoor VP (2007). Optimization of extraction and dyeing conditions for traditional turmeric dye, Indian J. Traditional Knowledge, 6(2): 270-278.

Samanta AK, Agarwal P, Singhee D, Datta S (2009). “ Natural dyes” eited by E. Perin. J. Text. Inst., 100(7) 565.

Samanta AK, Konar A, Chakroborty S, Datta S (2010). Dyeing of jute with tesu extract: part II thermodynamic parameters and kinetics of dyeing. J. Inst. Engg. (I), Text Engg; 91 P:7.

Shahid MAK, Kousar N, Akhtar N, Hussain T, Awan MS, Mubashir A, Bashir B, Javed A (2012). Dosimetric characterization of unknown dye poly vinyl alcohol films. J. Basic Appl. Sci., 8:508-512.

Shahid MAK, Mubashir A, Bashir B, Mansoor N (2013). Spectrophotometric analysis and gamma irradiation effects on dosimetric properties of Brassica oleracea dye aqueous solutions. Int. J. Chem. Mater. Sci., 1(8): 195-200.

Soutsas K (2010). Decolorization and degradation of reactive azo dyes via heterogeneous photocatalytic processes. Desalination. vol. 250, pp: 345- 350.

Tachikawa T, Handa C, Tokita S (2003). Sterilization of medical products, prime importance of radiation technology. J. Photopoly Sci. Tech., 16 P: 187.

Teli MD, Nayak AN, Nawathe VB, Adiivarekar RV (1994). "Dyeing of cotton with turmeric. University department of chemical Technology Bomby"

Tiwari HC, Singh P, Mishra PK, Srivastava P (2010). Pomegranate rind ultrasound and enzyme assisted extraction. Indian J. Fibre Text. Res., 35 (9) P:272.

Vaijapurkar SG (2008). Radiochromic techniques in radiation protection. Bull radiat Prtot, 31 P: 370.

Vajapurkar SG, Anuradha B (2010). Present status of Radiochromic techniques from nuclear radiation measurements. Indian J. Pure Appl. Phys., Vol 48, PP: 830-836.

Wang YN, Wang HX, Shen ZJ, Zhao LL, Clarke SR, Sun JH, Du YY, Shi GL (2009). Methyl palmitate, an acaricidal compound occurring in green walnut husks. J. Econ. Entomol., 102 (1), 196-202.

Wongcharee K, Meeyoo V, Chavadej S (2007). “Dye-sensitized solar cell using natural dyes extracted from rosella and blue pea flowers”, Sol. Energ. Mat. Sol. C 91 566-571.